nature microbiology

BRIEF COMMUNICATION

https://doi.org/10.1038/s41564-020-00830-7

Check for updates

Bacteriophage-resistant *Acinetobacter baumannii* are resensitized to antimicrobials

Fernando Gordillo Altamirano[1]✉, John H. Forsyth[1], Ruzeen Patwa[1], Xenia Kostoulias[2], Michael Trim[1], Dinesh Subedi[1], Stuart K. Archer[3], Faye C. Morris[2], Cody Oliveira[1], Luisa Kielty[1], Denis Korneev[1], Moira K. O'Bryan[1], Trevor J. Lithgow[2,4], Anton Y. Peleg[2,4,5] and Jeremy J. Barr[1,4]✉

We characterized two bacteriophages, ΦFG02 and ΦCO01, against clinical isolates of *Acinetobacter baumannii* and established that the bacterial capsule is the receptor for these phages. Phage-resistant mutants harboured loss-of-function mutations in genes responsible for capsule biosynthesis, resulting in capsule loss and disruption of phage adsorption. The phage-resistant strains were resensitized to human complement, beta-lactam antibiotics and alternative phages and exhibited diminished fitness in vivo. Using a mouse model of *A. baumannii* infection, we showed that phage therapy was effective.

A. baumannii is a top priority pathogen requiring urgent research and development of new therapeutic strategies[1–3], such as phage therapy[4,5] (expanded background information is presented in Supplementary Note 1). We isolated eight bacteriophages against a panel of clinical *A. baumannii* strains. Phages ΦFG02 and ΦCO01 and their hosts (strains AB900 and A9844, respectively) were chosen for further characterization. Microscopic examination of the phages suggested that ΦFG02 belongs to the *Myoviridae* family, and ΦCO01 belongs to the *Ackermannviridae* family of bacteriophages[6] (Fig. 1a) (complete phage characterization in Supplementary Notes 2 and 3, Extended Data Fig. 1a–g and Supplementary Fig. 1).

We observed the emergence of phage-resistant mutants when co-incubating strains AB900 and A9844 with their respective phages ΦFG02 and ΦCO01 (Extended Data Fig. 1f,g and Supplementary Fig. 2). We picked a single mutant of strain AB900 that was resistant to phage ΦFG02 (ΦFG02-R AB900) and a single mutant of strain A9844 that was resistant to phage ΦCO01 (ΦCO01-R A9844), and confirmed the phage-resistant phenotype using growth curves (Fig. 1b,c) and inverted spotting assays (Supplementary Fig. 2b,c).

Next, we compared the genomes of phage-resistant strains against the wild type, and identified a single-nucleotide deletion resulting in a frameshift in a gene within the K locus in both strains (Fig. 1d,e). Genes in the K locus of *A. baumannii* regulate the production, modification and export of capsular polysaccharides[7,8]. In ΦFG02-R AB900, the affected gene was *gtr29*, which codes for a glycosyltransferase, and in ΦCO01-R A9844 it was *gpi*, which codes for the enzyme glucose-6-phosphate isomerase[8]. Scanning electron microscopy (SEM) analysis suggested that the surface of the wild-type strains included a capsule, whereas there was no capsule on the surface of the phage-resistant strains (Fig. 1f and Supplementary Fig. 3). Defective capsule production was confirmed using Maneval's stain and a quantitative assay (Extended Data Fig. 2a–c), and was associated with impaired biofilm formation (Extended Data Fig. 2f,g). We screened an additional 24 independently evolved phage-resistant *A. baumannii* strains and determined that loss of capsule occurred in 20 out of 24 of these strains (Extended Data Fig. 2d,e). Together, these findings indicate a major defect in the overall production of capsule polysaccharides in the phage-resistant *A. baumannii* strains.

To demonstrate that the identified mutations were responsible for the phage-resistant phenotype, we disrupted the *gtr29* gene in AB900 and the *gpi* gene in A9844. The *Δgtr29* AB900 and *Δgpi* A9844 strains were completely resistant to phages ΦFG02 and ΦCO01, respectively (efficiency of plating (EOP) = 0%), and complementation restored phage susceptibility (EOP = 100%). Using an adsorption assay (Fig. 1g,h) we showed that more than 99% of ΦFG02 particles and 97% of ΦCO01 particles adsorbed to their respective wild-type hosts. By contrast, there was no phage adsorption for either the phage-resistant or knockout mutants, and adsorption was reinstated in the plasmid-complemented strains. Thus *A. baumannii* capsular polysaccharides are the phage receptors for ΦFG02 and ΦCO01 and phage resistance arose through alteration or loss of these receptors, leading to inhibition of phage adsorption.

Capsules are major determinants of virulence in *A. baumannii*[9,10]. They have a role in bacterial pathogenesis, enabling *A. baumannii* to evade components of the host immune response and to resist the effects of several antibiotics. We hypothesized that our capsule-deficient mutants had become vulnerable to the action of various antimicrobial agents. Therefore, we first determined their susceptibility profile to nine clinically relevant antibiotics (Fig. 2a; raw data of triplicates in Supplementary Table 1). ΦFG02-R AB900 exhibited a 16× decrease in the minimum inhibitory concentration (MIC) of ceftazidime relative to the wild type, becoming clinically sensitive to it, and a 2× decrease in the MIC of other beta-lactams and the fluoroquinolone ciprofloxacin. ΦCO01-R A9844 exhibited a 2× reduction in the MIC of minocycline, meropenem, cefepime and ampicillin with sulbactam. For cefepime and ampicillin with sulbactam, this resulted in a change of the clinical interpretation of the MIC, making A9844 sensitive to these antibiotics. Second, using a human serum killing assay, we demonstrated that wild-type strains withstood the action of the complement system, whereas

[1]School of Biological Sciences, Monash University, Clayton, Victoria, Australia. [2]Biomedicine Discovery Institute and Department of Microbiology, Monash University, Clayton, Victoria, Australia. [3]Monash Bioinformatics Platform, Faculty of Medicine, Nursing and Health Sciences, Monash University, Clayton, Victoria, Australia. [4]Centre to Impact AMR, Monash University, Clayton, Victoria, Australia. [5]Department of Infectious Diseases, The Alfred Hospital and Central Clinical School, Monash University, Clayton, Victoria, Australia. ✉e-mail: fernando.gordilloaltamirano@monash.edu; jeremy.barr@monash.edu

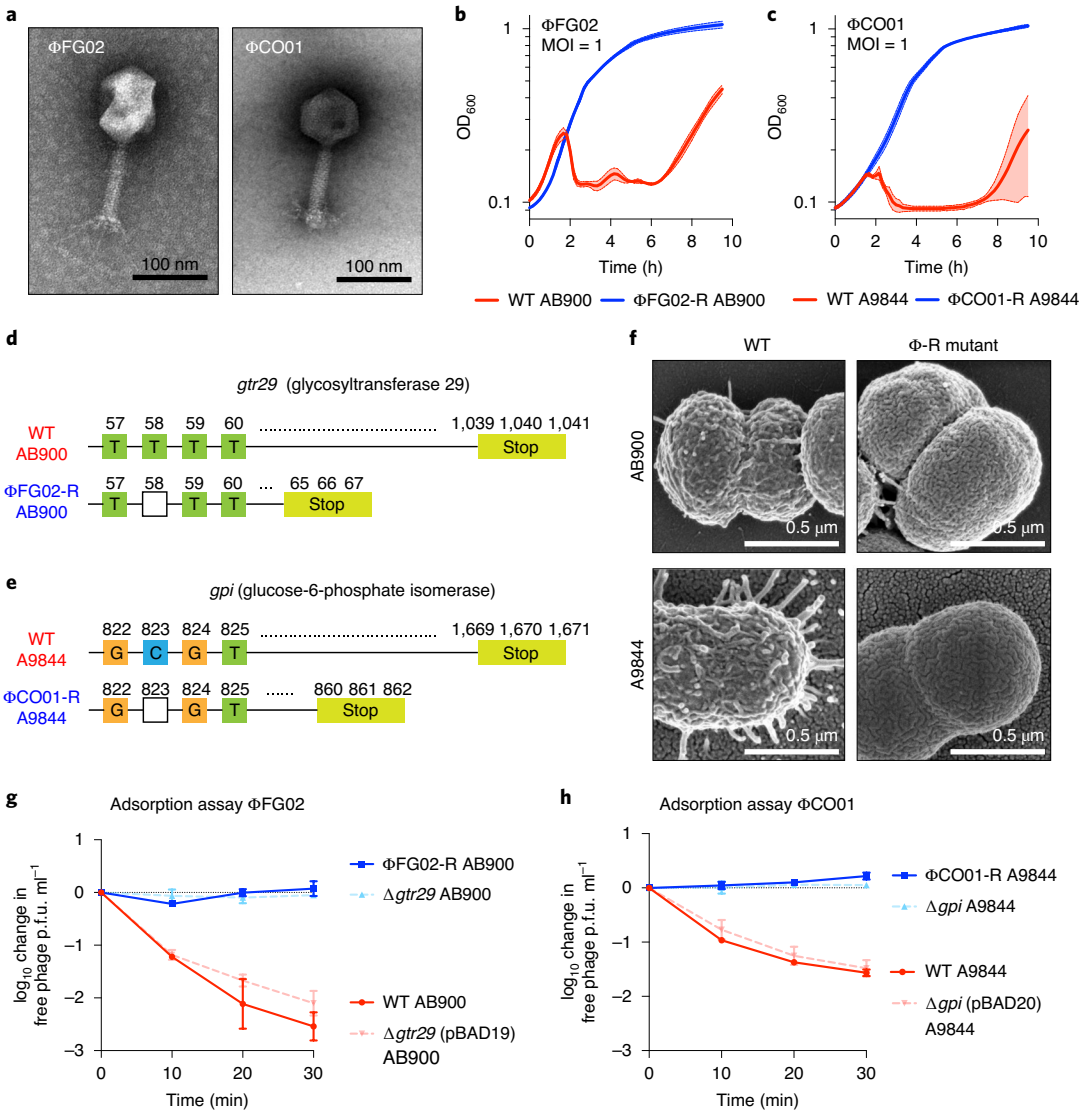

Fig. 1 | Bacteriophages, phage-resistant mutants and mechanism of phage resistance. a, Phage morphology of ΦFG02 and ΦCO01 visualized by transmission electron microscopy (TEM). **b**,**c**, Growth curves of wild-type (WT; red) and phage-resistant mutant (blue) *A. baumannii* in the presence of ΦFG02 (**b**) and ΦCO01 (**c**) at an MOI of 1. Data are mean ± s.d. ($n = 3$). OD_{600}, optical density at 600 nm. **d**,**e**, Mutations identified in ΦFG02-R AB900 (**d**) and ΦCO01-R A9844 (**e**) are found in the K locus and are associated with the phage-resistant phenotype. Numbers represent nucleotide position in the genes, box colours represent different nucleotides. Blank, deletion; yellow, stop codon. **f**, Cell surface appearance visualized by SEM suggests reduced capsule production in the phage-resistant (Φ-R) mutants (additional images in Supplementary Fig. 4). **g**,**h**, Phage adsorption assay on AB900 (**g**) and A9844 (**h**). Wild-type and plasmid-complemented (shades of red) and phage-resistant and knockout (shades of blue) mutant strains. Data are mean ± s.e.m. ($n = 3$).

phage-resistant mutants did not (Extended Data Fig. 3a). Third, we tested the phage-resistant mutants against our phage library and discovered instances of resensitization to phages that the strains were originally resistant to (Extended Data Fig. 3b). In summary, acquisition of phage resistance was accompanied by resensitization[11,12] to at least three different types of antimicrobial agents. This discovery is clinically relevant, as antibiotics, complement and phage all have a role in the clinical setting during the treatment of *A. baumannii* infections.

Next, we sought to observe the in vivo fitness of our phage-resistant mutants and their ability to invade and survive in mammalian hosts[9,10,13]. Using an established mouse model of bacteraemia (Methods), groups of BALB/c mice ($n = 4$) were infected with AB900, A9844 or their phage-resistant counterparts. After 8 h, the levels of bacterial colonization were assessed at four sites on the body of the mouse. In both strain pairs, we observed a 2-log reduction of bacterial load in solid organs and a more than 3-log reduction in blood for phage-resistant mutants, when compared with wild-type strains (Fig. 2b,c; Supplementary Note 4).

Finally, to gauge their translational potential, we tested phages ΦFG02 and ΦCO01 using the same in vivo model. One hour after infection, mice were treated with the corresponding phage at a multiplicity of infection (MOI) of 1 ($n = 4$ per group for AB900 with ΦFG02, $n = 3$ per group for A9844 with ΦCO01), or with PBS (untreated control). The length of follow-up was determined by the welfare of the control group, and was 12 h for AB900 and 8 h for A9844. Samples retrieved from phage-treated mice had significantly lower levels of bacteria than untreated mice, with ΦCO01 demonstrating stronger antibacterial activity (Fig. 2d,e, left and middle box plots). Furthermore, phage replication in vivo was

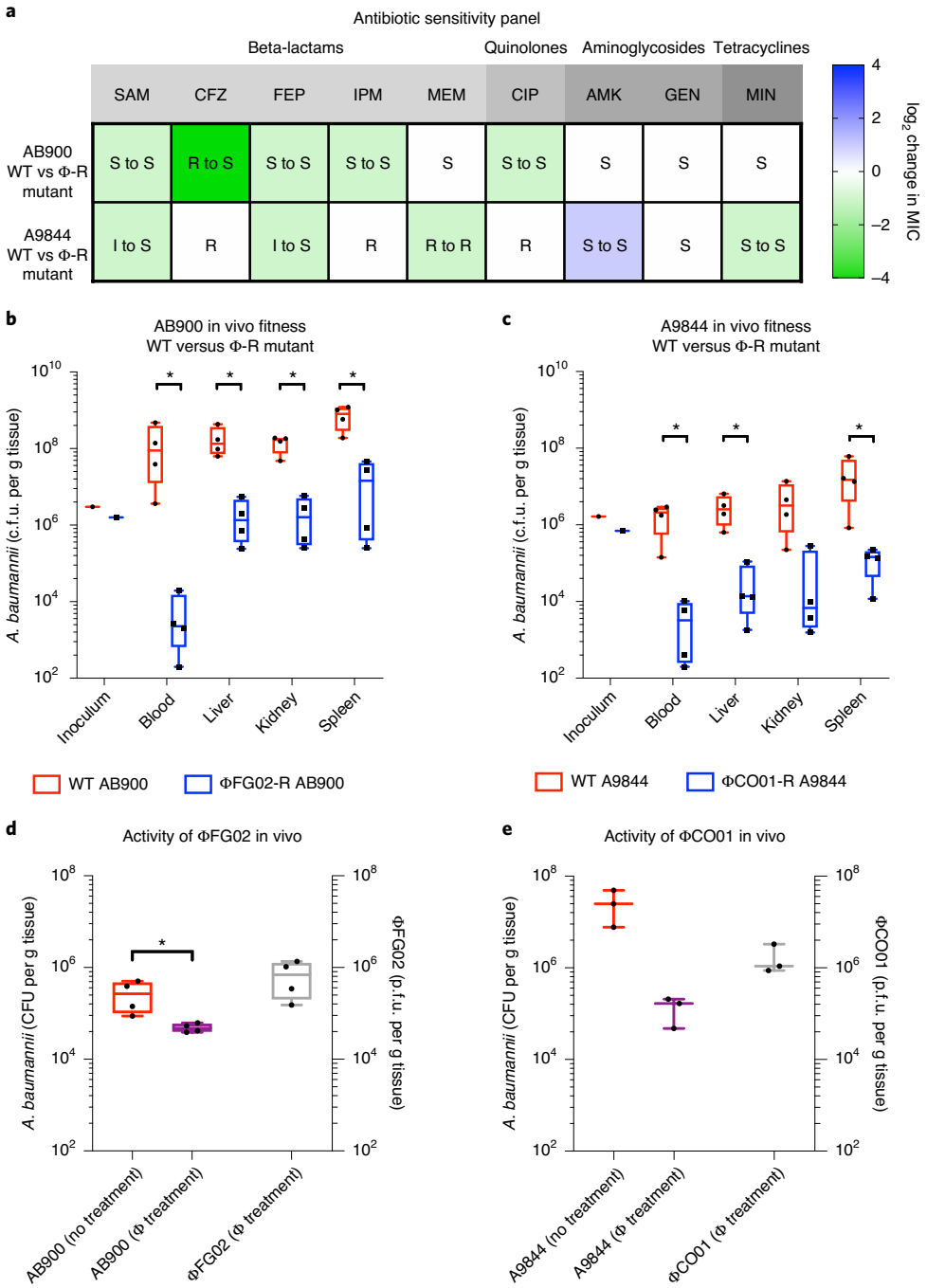

Fig. 2 | Antibiotic resensitization and in vivo assays. a, The MICs of 9 antibiotics measured using the microbroth-dilution method with the median ($n=3$) of the $\log_2$ change in MIC between the wild type and phage-resistant strains and the clinical interpretation of the MIC shown. S, sensitive; I, intermediate; R, resistant. Antibiotics: AMK, amikacin; CFZ, ceftazidime; CIP, ciprofloxacin; FEP, cefepime; GEN, gentamicin; IPM, imipenem; MEM, meropenem; MIN, minocycline; and SAM, ampicillin with sulbactam. **b**,**c**, In vivo fitness is reduced in phage-resistant *A. baumannii* AB900 (**b**) and A9844 (**c**) mutant strains. Bacterial burdens of wild-type and phage-resistant *A. baumannii*, per body site, at 8 h after infection, normalized by tissue weight. Each point represents data from one mouse ($n=4$; two-tailed Mann–Whitney test, $P=0.0286$ for all comparisons except kidney in A9844 ($P=0.0571$)). **d**,**e**, Phages ΦFG02 (**d**) and ΦCO01 (**e**) are effective against *A. baumannii* in vivo. Mice were treated with either phage or PBS. Box plots show bacterial burdens in untreated (left, red), and phage-treated (middle, purple) mice, as well as active phage particles (right, grey) in treated mice, normalized by tissue weight. In box plots, the centre line shows the median, box edges represent first and third quartiles and whiskers extend to extreme values. Each data point represents the average from four body sites from one mouse, ($n=4$, two-tailed Mann–Whitney test, $P=0.0286$ (AB900 and ΦFG02); $n=3$, two-tailed Mann–Whitney test, $P=0.1$ (A9844 and ΦCO01)). *$P<0.05$.

confirmed for ΦCO01 and suspected for ΦFG02 (Fig. 2d,e, right box plots and Supplementary Note 5; data by body site are presented in Supplementary Fig. 4).

In summary, we characterized ΦFG02 and ΦCO01, two phages that infect *A. baumannii* (further discussion in Supplementary Note 6). Despite the strong lytic activity of these phages, we

observed the rapid emergence of phage-resistant mutants in vitro. Phage-resistant strains harboured loss-of-function mutations in genes of the K locus, which are responsible for the biosynthesis of capsular polysaccharides. Using genetic engineering, we confirmed that disruption of *gtr29* in AB900 and *gpi* in A9844 led to phage resistance in these strains. We demonstrate that capsule loss in phage-resistant *A. baumannii* is associated with a reduction in biofilm formation, resensitization to antimicrobial agents including antibiotics, human complement and phages, and a reduction in fitness in a mouse model of bacteraemia. Finally, we preliminarily gauged the translational potential of phages ΦFG02 and ΦCO01 by observing their bactericidal activity in vivo.

Methods

Bacterial strains and plasmids. Supplementary Tables 2 and 3 contain a list of strains, plasmids and genomes used in this study.

Phage isolation and purification. Phages were isolated from raw sewage samples. Aliquots of sewage were combined with overnight cultures of up to three bacterial strains, and supplemented with 10× LB and 10 mM $CaCl_2$ and $MgSO_4$. Mixtures were incubated overnight and the resulting lysates were purified with the previously described Phage-on-Tap protocol[14].

Transmission electron microscopy. Ten-microlitre droplets of phage suspension were placed on copper TEM grids (200 mesh; SPI) with carbon-coated ultrathin formvar film[15]. They were left for 30 s and then dried using filter paper. Negative staining was performed with a uranyl acetate water solution (1% w/v) and the grids were examined under a transmission electron microscope (JEM-1400 Plus) at an accelerating voltage of 80 kV.

Phage adsorption assay. Bacteria from overnight cultures and phages from pure lysates were mixed at an MOI of 0.01 (inoculum of 10^8 colony-forming units (c.f.u.) per ml) in LB. The suspensions were incubated at 37 °C with aeration. At each time point, samples of the suspensions were transferred into chloroform-saturated PBS, vortexed, and then centrifuged at 3,500*g* for 3 min. The supernatant was diluted in PBS and plated in duplicate for quantification of free phage particles.

Isolation of phage-resistant *A. baumannii* mutants. Following the same principle as the spot assay, 25 µl aliquots of pure lysate (concentration > 10^8 plaque-forming units (p.f.u.) ml^{-1}) were spotted onto bacterial lawns. After an overnight incubation, bacterial colonies growing in the middle of lysis zones were picked and streaked onto LB agar plates for two rounds of single-colony isolation. The phage-resistant phenotypes were confirmed using three methods: inverted spot plate assays[16], standard soft-agar overlay assays, and in vitro growth curves.

Extraction of bacterial genomic DNA, sequencing and bacterial genome comparison. The GenElute Bacterial Genomic DNA Kit protocol (Sigma-Aldrich) was used for DNA extraction. Sequencing was performed using the Illumina HiSeq 150 bp paired-end platform (Genewiz). The genomes of AB900, A9844 and their phage-resistant counterparts, were independently assembled from these reads and compared with the pipeline described in Supplementary Methods.

Gene knockout and complementation. Supplementary Table 4 contains the primers used in this section of the study. Genes of interest were disrupted and complemented back using a variation of the methods described previously[17]. Further details are provided in Supplementary Methods.

SEM for capsule observation. A 20-µl droplet of five-times PBS-washed bacterial suspension was placed onto a fresh gold-coated silicon wafer and the cells were allowed to settle for 5 min, followed by washing with PBS. The wafer was then placed in 2.5% glutaraldehyde in PBS for 15 min, washed with deionized water and dehydrated by immersing in increasing concentrations of ethanol for 3 min each. Residual ethanol was removed with a critical-point dryer CPD 030 (BAL-TEC). The sample was mounted on a standard metal SEM stub and then coated with an approximately 10-nm-thick gold layer using a sputter coater (SCD 005; BAL-TEC). The samples were examined under high vacuum in the FE-SEM ThermoFisher Elstar G4 at an accelerating voltage of 2 kV, in secondary electron mode, with a working distance of 4 mm, operating in immersion mode with the through lens detector.

Antibiotic susceptibility assay. MICs of nine antibiotics were assessed using the microbroth-dilution protocol as previously described[18] and interpreted using the cut-off values from the Clinical and Laboratory Standard Institute[19]. The antibiotics tested were amikacin, ceftazidime, ciprofloxacin, cefepime, gentamicin, imipenem, meropenem, minocycline and ampicillin + sulbactam.

Mouse experiments and ethics. Three to four female, 6- to 10-week-old BALB/c mice were used per group. The sample size was selected on the basis of ethics considerations, and was sufficient to support the research hypotheses. Mice were randomly allocated to the different experimental groups and, due to the small scale of the experiment, no blinding procedures were performed. Bacterial inoculums of either wild-type or phage-resistant *A. baumannii* were prepared to a concentration of 10^6 c.f.u. in 100 µl PBS. Before administration, the bacterial suspensions were mixed in a 1:1 ratio with 6% porcine stomach mucin (Sigma-Aldrich) in PBS, for a total volume of 200 µl, and mice were injected intraperitoneally. Treatment consisted of intraperitoneal injection of either phage suspensions in PBS at an MOI of 1, PBS alone, or no treatment (for the bacterial fitness assays). Mice were followed for up to 12 h, with the end point decided on the basis of animal wellbeing in any of the groups being compared. At the humane end point, blood was extracted through cardiac puncture and a laparotomy was performed to obtain a section of the liver, right kidney and spleen. The organs were weighed and then homogenized in PBS. Blood and organ suspensions were then serially diluted in PBS for c.f.u. quantification. In mice that received phage treatment, the blood and organ suspensions were pelleted by centrifugation, and the supernatant was serially diluted and plated with the soft-agar overlay assay for p.f.u. quantification. All protocols involving mice were reviewed and approved by the AMREP Animal Ethics Committee (Project ID: E/1689/2016/M) and complied with the National Health and Medical Research Council guidelines. Mice were housed at the Monash Animal Research Facility, Monash University.

Statistics and reproducibility. Results from TEM, SEM, capsule staining and phage plaque morphology are representative of at least 100 observations (single cells, phage virions, microscopy fields and plaques, respectively).

Reporting Summary. Further information on research design is available in the Nature Research Reporting Summary linked to this article.

Data availability

The genetic sequences acquired during this study have been deposited into the National Center for Biotechnology Information database as a BioProject under accession number PRJNA608808. The project contains data for *A. baumannii* strains AB900 (accession number SAMN14483301), A9844 (accession number SAMN14483302), ΦFG02-R AB900 (accession number SAMN14511297) and ΦCO01-R A9844 (accession number SAMN14511298). Phage genomes were independently submitted on GenBank (ΦFG02 accession number MT648818 and ΦCO01 accession number MT648819). Source data are provided with this paper.

Code availability

The study did not involve the creation of novel code for bioinformatics analyses. All the used software is freely accessible and is referenced in the Supplementary Information.

Received: 21 April 2020; Accepted: 10 November 2020;
Published online: 11 January 2021

References

1. *Antibiotic Resistance Threats in the United States* (Centers for Disease Control and Prevention, 2019); https://www.cdc.gov/drugresistance/biggest-threats.html
2. *Global Priority List of Antibiotic-Resistant Bacteria to Guide Research, Discovery, and Development of New Antibiotics* (World Health Organization, 2017); https://www.who.int/medicines/publications/WHO-PPL-Short_Summary_25Feb-ET_NM_WHO.pdf?ua=1
3. Peleg, A. Y., Seifert, H. & Paterson, D. L. *Acinetobacter baumannii*: emergence of a successful pathogen. *Clin. Microbiol. Rev.* **21**, 538–582 (2008).
4. Gordillo Altamirano, F. L. & Barr, J. J. Phage therapy in the postantibiotic era. *Clin. Microbiol. Rev.* **32**, e00066-18 (2019).
5. Schooley, R. T. et al. Development and use of personalized bacteriophage-based therapeutic cocktails to treat a patient with a disseminated resistant *Acinetobacter baumannii* infection. *Antimicrob. Agents Chemother.* **61**, e00954-17 (2017).
6. Ackermann, H.-W. in *Advances in Virus Research* Vol. 82 (eds M. Łobocka & W. T. Szybalski) 1–32 (Academic Press, 2012).
7. Kenyon, J. J. & Hall, R. M. Variation in the complex carbohydrate biosynthesis loci of *Acinetobacter baumannii* genomes. *PLoS ONE* **8**, e62160 (2013).
8. Singh, J. K., Adams, F. G. & Brown, M. H. Diversity and function of capsular polysaccharide in *Acinetobacter baumannii*. *Front. Microbiol.* **9**, 3301 (2019).
9. Morris, F. C., Dexter, C., Kostoulias, X., Uddin, M. I. & Peleg, A. Y. The mechanisms of disease caused by *Acinetobacter baumannii*. *Front. Microbiol.* **10**, 1601 (2019).
10. Geisinger, E., Huo, W., Hernandez-Bird, J. & Isberg, R. R. *Acinetobacter baumannii*: envelope determinants that control drug resistance, virulence, and surface variability. *Annu. Rev. Microbiol.* **73**, 481–506 (2019).

11. Torres-Barceló, C. & Hochberg, M. E. Evolutionary rationale for phages as complements of antibiotics. *Trends Microbiol.* **24**, 249–256 (2016).
12. Chan, B. K. et al. Phage selection restores antibiotic sensitivity in MDR *Pseudomonas aeruginosa*. *Sci. Rep.* **6**, 26717 (2016).
13. Russo, T. A. et al. The K1 capsular polysaccharide of *Acinetobacter baumannii* strain 307-0294 is a major virulence factor. *Infec. Immun.* **78**, 3993–4000 (2010).
14. Bonilla, N. et al. Phage on tap—a quick and efficient protocol for the preparation of bacteriophage laboratory stocks. *PeerJ* **4**, e2261 (2016).
15. Davison, E. & Colquhoun, W. Ultrathin formvar support films for transmission electron microscopy. *J. Electron Microsc. Tech.* **2**, 35–43 (1985).
16. Gillis, A. & Mahillon, J. An improved method for rapid generation and screening of *Bacillus thuringiensis* phage-resistant mutants. *J. Microbiol. Methods* **106**, 101–103 (2014).
17. Datsenko, K. A. & Wanner, B. L. One-step inactivation of chromosomal genes in *Escherichia coli* K-12 using PCR products. *Proc. Natl Acad. Sci. USA* **97**, 6640–6645 (2000).
18. Wiegand, I., Hilpert, K. & Hancock, R. E. Agar and broth dilution methods to determine the minimal inhibitory concentration (MIC) of antimicrobial substances. *Nat. Protoc.* **3**, 163–175 (2008).
19. *Performance Standards for Antimicrobial Susceptibility Testing; Twenty-Fifth Informational Supplement Document M100-S25* (Clinical and Laboratory Standards Institute, 2015).

Acknowledgements

We thank L. Perlaza-Jiménez and R. Dunstan for expert advice in the early stage of this project; the Monash Ramaciotti Cryo-EM platform for the use of facilities; A. Fulcher and A. de Marco for granting access to the SEM; C. Vásconez for feedback regarding the readability, clarity and structure of the manuscript; and D. McCarthy for raw sewage samples for phage isolation. F.G.A. acknowledges the support from Monash University through the Monash Postgraduate Research Scholarships funding his doctoral studies. T.J.L. is an ARC Australian Laureate Fellow (FL130100038). This work, including the efforts of J.J.B., was funded by the Australian Research Council (ARC) Discovery Early Career Researcher Award (DECRA) (DE170100525), National Health and Medical Research Council (NHMRC: 1156588) and the Perpetual Trustees Australia award (2018HIG00007).

Author contributions

F.G.A., T.J.L., A.Y.P. and J.J.B. conceived the study. F.G.A., M.T., C.O. and L.K. performed phage isolation. F.G.A. and D.S. performed phenotypic and genotypic characterization of phages. J.H.F., R.P. and F.C.M. planned and performed knockout and complementation experiments. D.K. performed TEM and SEM. S.K.A. performed bioinformatics analyses of bacterial genomes. F.G.A. performed most of the in vitro characterization of phage-resistant mutants, with help from J.H.F. (capsule, biofilm and antibiotic assays) and M.T. (biofilm assays). F.G.A. and X.K. performed in vivo experiments. M.K.O., T.J.L., A.Y.P. and J.J.B. provided resources for experimental work. T.J.L., A.Y.P. and J.J.B. supervised and funded the project. F.G.A. and J.J.B. wrote the original draft. All authors were involved in reviewing and editing the final manuscript.

Competing interests

The authors declare no competing interests.

Additional information

Extended data is available for this paper at https://doi.org/10.1038/s41564-020-00830-7.

Supplementary information is available for this paper at https://doi.org/10.1038/s41564-020-00830-7.

Correspondence and requests for materials should be addressed to F.G.A. or J.J.B.

Peer review information *Nature Microbiology* thanks the anonymous reviewers for their contribution to the peer review of this work. Peer reviewer reports are available.

Reprints and permissions information is available at www.nature.com/reprints.

Publisher's note Springer Nature remains neutral with regard to jurisdictional claims in published maps and institutional affiliations.

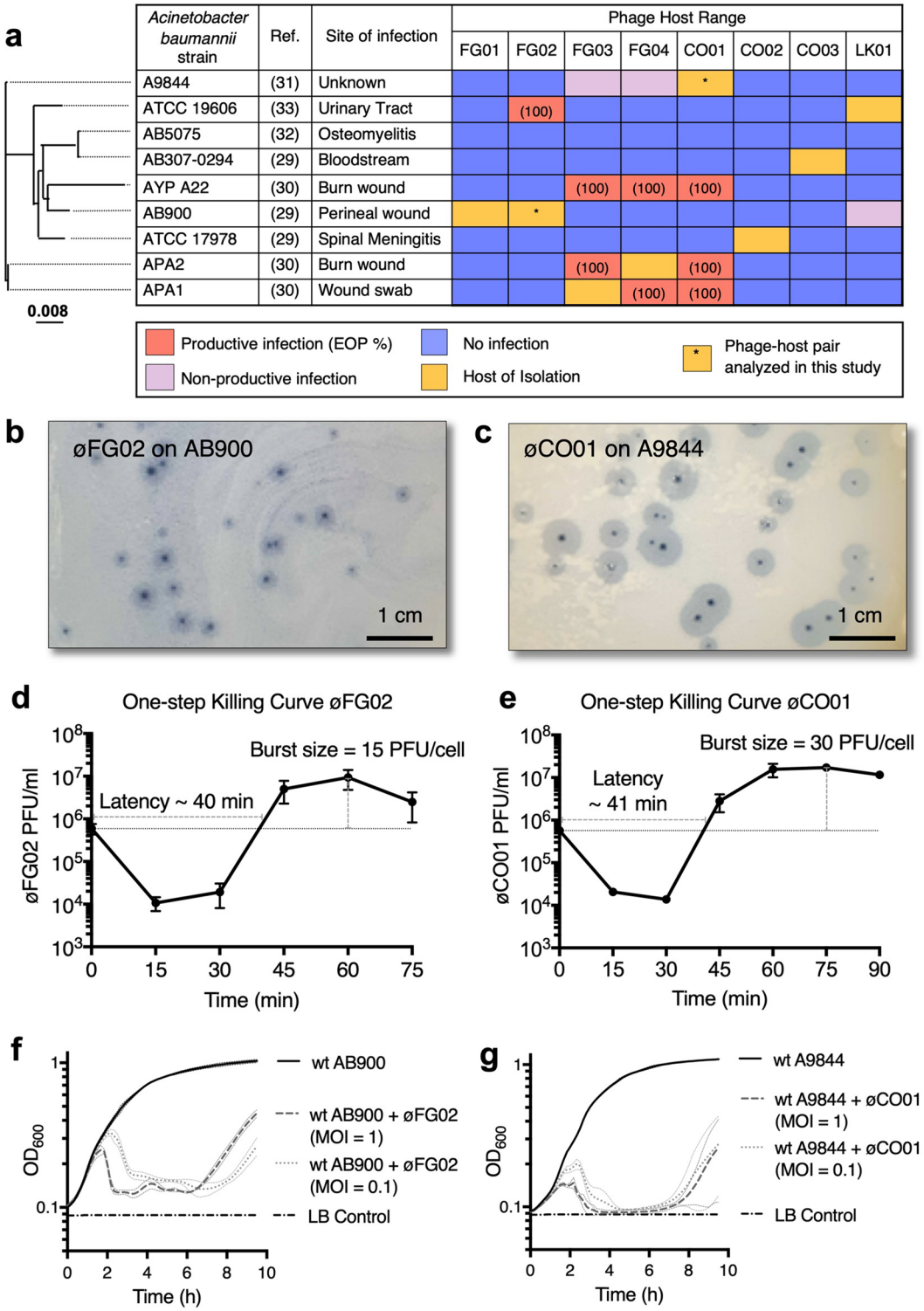

Extended Data Fig. 1 | Characterization of *Acinetobacter baumannii*-specific phages. a, Host range of the eight *A. baumannii*-specific phages isolated in this study. Bacterial strains are ordered by the core-genome alignment phylogenetic tree on the left. Productive infection is defined as lysis on a spot assay and production of plaques on a soft agar overlay, whereas non-productive infection is defined as lysis on a spot assay with no plaques on a soft overlay agar. Efficiency of plating (EOP) is reported as a percentage compared to the host of isolation. **b**,**c**, Plaque morphology of phage øFG02 on host AB900 and øCO01 on host A9844, showing the central clearings or lysis zones surrounded by hazy halos. Scale bars: 1 cm. **d**,**e**, One-step killing curves of phages øFG02 and øCO01 on their hosts of isolation. Latency time was measured from the beginning of the experiment to when the curve at exponential growth reached the initial phage inoculum, whereas burst size was calculated by dividing the maximum free phage count after bacterial burst by the initial phage titer in the experiment. Data are mean ± s.e.m. ($n = 3$). **f**,**g**, Growth curves of *A. baumannii* strains AB900 and A9844 with and without phages. Phages were applied at two different multiplicities of infection (1 and 0.1). Lytic activity of phages is shown by the drop in optical density shortly after initiation of the bacterial exponential growth phase; and emergence of phage resistance is shown after 6 h of incubation. Data are mean ± s.d. ($n = 3$). OD_{600}, optical density at 600 nm.

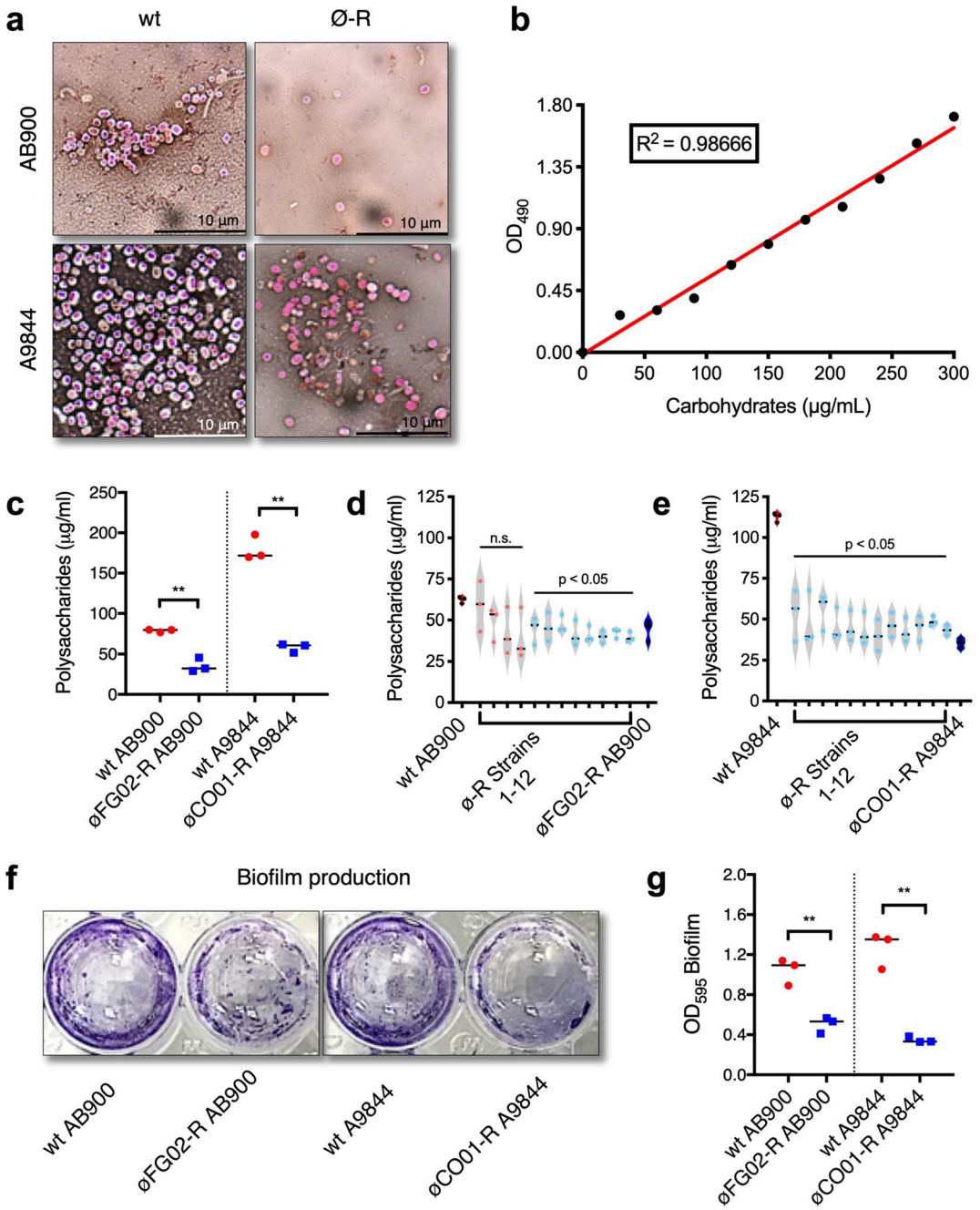

Extended Data Fig. 2 | Reduced capsule and biofilm production in phage-resistant mutants. a, Microscopic inspection of capsule thickness in slides stained using the Maneval's technique. Scale bars: 10 µm. **b**, Standard curve for the phenol-chloroform capsule quantification assay, calibrated with carbohydrate standards ranging from 0 to 300 µg/ml. OD_{490}, optical density at 490 nm. **c**, Production of capsule polysaccharides ($n = 3$), for AB900 vs. øFG02-R AB900: 79 ± 1.7 µg/ml vs. 35.6 ± 8.8 µg/ml (mean ± s.d.), $P = 0.001$; and for A9844 vs. øCO01-R A9844: 179.9 ± 15.6 µg/ml vs. 58.1 ± 5.6 µg/ml; $P = 0.0002$. **d**,**e**, Repeatability of phage-resistance evolution was assessed by measuring capsule production of twelve independently-evolved phage-resistant strains from each of the wild type hosts (AB900 and A9844). Violin plots (n = 3) of surface polysaccharides produced by each strain compared between the wild type host and each of the additional phage-resistant mutants. **f**,**g**, Biofilm production on a polystyrene surface at 48 h, measured by absorbance of crystal-violet stained and ethanol-solubilized biofilm ($n = 3$); optical density of biofilm 1 ± 0.1 vs. 0.5 ± 0.1 (mean ± s.d.), $P = 0.0038$, for AB900 vs. øFG02-R AB900; and 1.3 ± 0.2 vs. 0.4 ± 0.03, $P = 0.001$, for A9844 vs. øCO01-R A9844. For panels C, D, E and G, wild type strains represented in red and (original) phage-resistant mutants in blue, bars represent medians, each point represents the average from three technical replicates, and P values pertain to unpaired t tests, two-tailed. ** = $P < 0.005$; n.s. = non-significant.

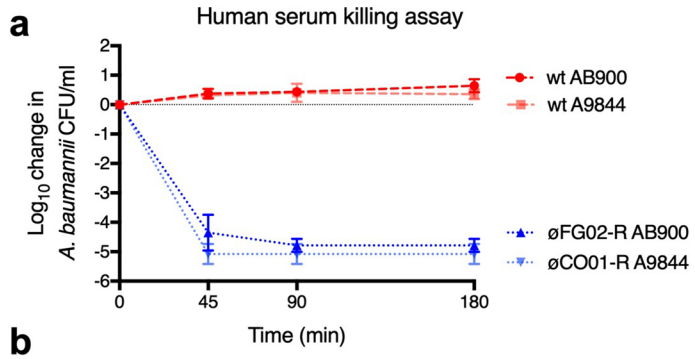

b

Acinetobacter baumannii strain	Expanded Phage Host Range							
	FG01	FG02	FG03	FG04	CO01	CO02	CO03	LK01
wt AB900								
øFG02-R AB900	(100)							(100)
wt A9844								
øCO01-R A9844	(1)							(0.1)

No infection | Non-productive infection | Productive infection (EOP %)

Extended Data Fig. 3 | Further resensitization of phage-resistant *A. baumannii* to antimicrobials. a, Human serum killing assay. Freshly-thawed human serum was inoculated with 10^5 CFU ml^{-1} of *A. baumannii*, and the change in bacterial load was measured at regular intervals. Wild type strains (shades of red) grew in serum whereas phage-resistant strains (shades of blue) were rapidly killed. Data are mean ± s.e.m. ($n = 3$). **b**, Expanded phage host range map of the *A. baumannii*-specific phage library against øFG02-R AB900 and øCO01-R A9844 reveals sensitization to additional phages. Efficiency of plating (EOP) is reported as a percentage compared to the host of isolation.

nature research

Corresponding author(s): Jeremy J. Barr

Last updated by author(s): 2020/11/06

Reporting Summary

Nature Research wishes to improve the reproducibility of the work that we publish. This form provides structure for consistency and transparency in reporting. For further information on Nature Research policies, see our Editorial Policies and the Editorial Policy Checklist.

Statistics

For all statistical analyses, confirm that the following items are present in the figure legend, table legend, main text, or Methods section.

n/a	Confirmed	
☐	☒	The exact sample size (*n*) for each experimental group/condition, given as a discrete number and unit of measurement
☐	☒	A statement on whether measurements were taken from distinct samples or whether the same sample was measured repeatedly
☐	☒	The statistical test(s) used AND whether they are one- or two-sided *Only common tests should be described solely by name; describe more complex techniques in the Methods section.*
☒	☐	A description of all covariates tested
☒	☐	A description of any assumptions or corrections, such as tests of normality and adjustment for multiple comparisons
☐	☒	A full description of the statistical parameters including central tendency (e.g. means) or other basic estimates (e.g. regression coefficient) AND variation (e.g. standard deviation) or associated estimates of uncertainty (e.g. confidence intervals)
☒	☐	For null hypothesis testing, the test statistic (e.g. *F*, *t*, *r*) with confidence intervals, effect sizes, degrees of freedom and *P* value noted *Give P values as exact values whenever suitable.*
☒	☐	For Bayesian analysis, information on the choice of priors and Markov chain Monte Carlo settings
☒	☐	For hierarchical and complex designs, identification of the appropriate level for tests and full reporting of outcomes
☒	☐	Estimates of effect sizes (e.g. Cohen's *d*, Pearson's *r*), indicating how they were calculated

Our web collection on statistics for biologists contains articles on many of the points above.

Software and code

Policy information about availability of computer code

Data collection

Microsoft Excel v16.20
Biotek Gen5 v3.0
MinKNOW v1.7.14
Illumina sequencing was outsourced (performed at Genewiz)

Data analysis	GraphPad Prism v7.0 Deepbinner v0.2.0 Trimmomatic v.039 Unicycler v0.4.3 (64) RAST v2.0 PHASTER VIBRANT v1.2.1 Trimviz Burrows-Wheeler Aligner RNAsik v1.5.0 samtools mpileup v1.8 Varscan2 v2.4.0 IGV v2.3.59 Prokka v.1.13.7 Roary v3.11.2 RAXML v8.2.12 APE v5.3

For manuscripts utilizing custom algorithms or software that are central to the research but not yet described in published literature, software must be made available to editors and reviewers. We strongly encourage code deposition in a community repository (e.g. GitHub). See the Nature Research guidelines for submitting code & software for further information.

Data

Policy information about availability of data

All manuscripts must include a data availability statement. This statement should provide the following information, where applicable:

- Accession codes, unique identifiers, or web links for publicly available datasets
- A list of figures that have associated raw data
- A description of any restrictions on data availability

The genetic sequences acquired during this study have been deposited into the National Center for Biotechnology Information database as a BioProject (accession number PRJNA608808). The project contains data for A. baumannii strains AB900 (accession number SAMN14483301), A9844 (accession number SAMN14483302), øFG02-R AB900 (accession number SAMN14511297) and øCO01-R A9844 (accession number SAMN14511298). Phage genomes were independently submitted on GenBank (øFG02 accession number MT648818 and øCO01 accession number MT648819).
Source data has been provided for all growth curve, phage dynamics, capsule, biofilm, complement system, and in vivo experiments, in three Excel documents (for Figure 1, Figure 2, and Supplementary Figures, respectively).
Raw data of triplicates on antibiotic sensitivity experiments (Fig. 2A) has been provided as Supplementary Table 1.

Field-specific reporting

Please select the one below that is the best fit for your research. If you are not sure, read the appropriate sections before making your selection.

☒ Life sciences ☐ Behavioural & social sciences ☐ Ecological, evolutionary & environmental sciences

For a reference copy of the document with all sections, see nature.com/documents/nr-reporting-summary-flat.pdf

Life sciences study design

All studies must disclose on these points even when the disclosure is negative.

Sample size	No sample-size calculation was performed. The sample size of n=3 for animal models was selected based on ethics considerations, and was sufficient to support the research hypothesis.
Data exclusions	No data were excluded.
Replication	Experimental work was replicated in at least 3 biological samples with 2 technical measurements each. The established protocols and techniques were successfully applied by different researchers. The isolation of phage-resistant mutants and knockout/complementation of bacterial strains were not repeated due to experimental complexity and costs.
Randomization	Organisms were randomly assigned to experimental groups in the animal models.
Blinding	Blinding was not relevant to the animal models in our study due to the small scale of the experiment.

Reporting for specific materials, systems and methods

We require information from authors about some types of materials, experimental systems and methods used in many studies. Here, indicate whether each material, system or method listed is relevant to your study. If you are not sure if a list item applies to your research, read the appropriate section before selecting a response.

Materials & experimental systems

n/a	Involved in the study
☒	☐ Antibodies
☒	☐ Eukaryotic cell lines
☒	☐ Palaeontology and archaeology
☐	☒ Animals and other organisms
☒	☐ Human research participants
☒	☐ Clinical data
☒	☐ Dual use research of concern

Methods

n/a	Involved in the study
☒	☐ ChIP-seq
☒	☐ Flow cytometry
☒	☐ MRI-based neuroimaging

Animals and other organisms

Policy information about studies involving animals; ARRIVE guidelines recommended for reporting animal research

Laboratory animals	Mus musculus (house mouse), BALB/c, female, 4-to-6 weeks old
Wild animals	The study did not involve wild animals.
Field-collected samples	The study did not involve samples collected from the field.
Ethics oversight	All protocols involving animals were reviewed and approved by the Monash University Animal Ethics Committee (Project ID: E/1689/2016/M) and complied with the National Health and Medical Research Council guidelines. Animals were housed at the Monash Animal Research Facility, Monash University.

Note that full information on the approval of the study protocol must also be provided in the manuscript.